SEMARAK ILMU PUBLISHING
202103268166(003316878-P)

Journal of Advanced Research in Applied Sciences and Engineering Technology

Journal homepage:
https://semarakilmu.com.my/journals/index.php/applied_sciences_eng_tech/index
ISSN: 2462-1943

Quantum Entanglement in Nonlinear Coupler with Raman Process

Mohd Syafiq Mohd Hanapi[1], Abdel-Baset Mohamed Abdelhamid Ibrahim[1,*], Ahmad Musleh Alrub[2], Pankaj Kumar Choudhury[3]

[1] Faculty of Applied Sciences, Universiti Teknologi MARA (UiTM), 40450 Shah Alam, Selangor, Malaysia
[2] Department of Physics, Al-Hussein Bin Talal University, Ma'an 71111, Jordan
[3] International Research Center for Advanced Photonics, Zhejiang University, Building 1A, 718 East Haizhou Rd., Haining, Zhejiang 314400, P.R. China

ARTICLE INFO

Article history:
Received
Received in revised form
Accepted
Available online

Keywords:
Quantum optics; nonlinear coupler; Raman process; quantum entanglement

ABSTRACT

This paper examines the possible quantum entanglement generated in a coupler system consisting of two waveguides, where one waveguide is nonlinear and Raman-active, while the other waveguide only undergoes linear processes. The analytical-perturbative method is employed to investigate the production of entangled states in the given system. The Hillery-Zubairy criterion is employed to examine the possible quantum entanglement between the two fundamental pump modes propagating in both waveguides. We explore the generation of quantum entanglement under different initial conditions and critical design parameters. The simulation results suggest a continuous entanglement that remains until a particular distance of interaction is reached. As the linear coupling parameter increases, the relationship between the maximum reachable distance for entanglement and the degree of entanglement becomes more complex. The study reveals that entanglement experiences significant fluctuations when there is a substantial frequency mismatch between the modes.

1. Introduction

In today's era of rapid technological advancement, relying solely on classical technology is no longer adequate. Classical technology has inherent limitations that cannot be avoided. As computational tasks become increasingly complex, classical technology is proving to be inefficient in solving them [1]. With the rapid advancement of computer technology, classical security measures are becoming increasingly inadequate. For example, compared to quantum cryptography, classical technology is unable to provide the same level of reliable security features [2]. As technology advances rapidly, there is a growing need to replace classical technology with the more superior quantum technology.

One of the fundamental concepts of quantum mechanics that has the potential to impact quantum technology is quantum entanglement. Quantum entanglement is the phenomenon in which two or more particles are inexplicably interconnected. This connection will persist even if the Second

* *Corresponding author.*
E-mail address: abdelbaset@uitm.edu.my

https://doi.org/10.37934/araset.57.1.3343

correlated particles are separated by a very great distance. When two particles are entangled, any change to one particle will affect the other particle. Quantum entanglement has numerous current and potential future applications across various fields. For example, in quantum communication, quantum entanglement enables secure communication through quantum key distribution (QKD) [3, 4]. By encoding information in entangled particles, such as photons, it becomes impossible for an eavesdropper to intercept the information without disturbing the entanglement. This has the potential to revolutionize cryptography and provide unhackable communication channels. Quantum entanglement is also a crucial resource for quantum computers [5]. By entangling qubits, quantum computers can perform parallel computations and solve certain problems exponentially faster than classical computers [6]. While quantum entanglement holds great promise for these applications, many are still in the early stages of development and require significant technological advancements before becoming widely available. However, ongoing research in the field of quantum physics continues to push for more efficient sources of entangled light.

Quantum properties of light can be generated in various nonlinear systems, such as Bose-Einstein condensate [7] and optical parametric amplifiers [8]. Among these, the nonlinear coupler has caught the interest of many researchers due to its advantages as a simple-structured, experimentally realizable, and simply integrated device [9, 10]. The standard two-waveguide coupler system is essentially two codirectional waveguides placed in close proximity to each other to allow for the coupling between the optical field modes via the evanescent field waves. Each waveguide is pumped with a single optical mode. Various types of nonlinear couplers have been extensively studied in the literature, including three-waveguide couplers [11, 12], four-waveguide couplers [13, 14], and cavity-assisted nonlinear couplers [15, 16]. Additionally, nonlinear couplers based on different nonlinear processes, such as the Kerr effect [17-20] and second harmonic generation [21], have also been proposed.

The Raman effect is one of the most promising methods for generating nonclassical light. The Raman process happens as a result of the interaction of light with some solid and is a nonlinear scattering process of the third order [22]. As shown in Figure 1(a), there are two possible outcomes of this interaction: Stokes Raman scattering and anti-Stokes Raman scattering, both of which involve the transfer of energy from light to the solid. When the energy of the radiated light is less than that of the incident light, Stokes Raman scattering takes place. When the emitted light's energy is greater than the incident light's, an effect known as anti-Stokes Raman scattering occurs. In addition, phonon vibrations in materials will be induced by both processes. Quantum opticians have been interested in the quantum description of many types of the Raman process in nonlinear media (see, e.g., [23]).

To the best of our knowledge, the quantum properties of Raman nonlinear couplers remain rather limited, with only two published articles providing insights so far. This is likely due to the mathematical and numerical rigor required for this type of work. The first study investigates the behavior of squeezing and sub-Poissonian photon statistics in a Raman nonlinear coupler composed of two waveguides operating via the Raman process [24]. The second study explores the quantum Zeno effect in an asymmetric Raman nonlinear coupler configuration, where one waveguide is linear while the other employs a nondegenerate hyper-Raman process [25]. The main objective of the current study is to explore another fundamental quantum property-quantum entanglement. The investigation of entanglement in Raman nonlinear coupler devices represents a domain yet to be extensively explored.

In this article, we look at a two-waveguide coupler system with one nonlinear Raman-active waveguide connected to another waveguide with just a linear process. One fundamental coherent mode is pumped into each waveguide. When the coherent fundamental mode is pumped into the Raman-active waveguide, it generates Raman Stokes, anti-Stokes, and phonon modes (see Figure

1(b)). Both waveguide's fundamental modes are also linearly connected (cross-action coupling) by evanescent waves. We will investigate how quantum entanglement is generated in the current system under various initial conditions and critical design parameters. For clarity, we shall refer to the light mode injected into the Raman-active waveguide as the 'first mode' and the mode inserted into the linear waveguide as the 'second mode' throughout this paper.

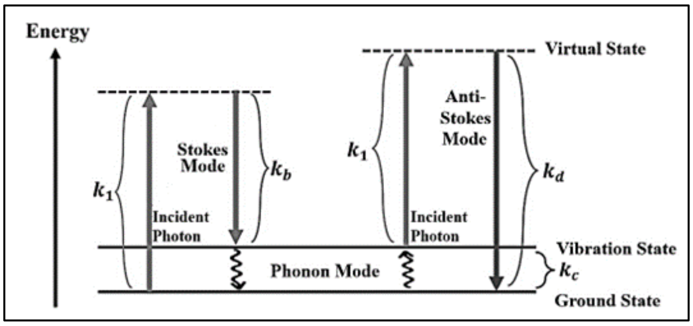

(a)

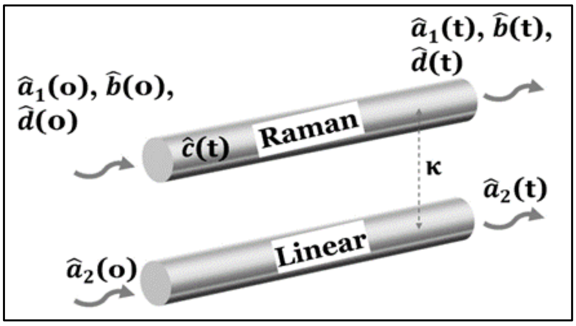

(b)

Fig. 1. (a) Diagram for Raman process (b) Basic diagram of the two-waveguide asymmetric nonlinear coupler

2. Mathematical Description of the System

To investigate the quantum entanglement in the current system, we employ the analytical perturbative (AP) method. Sen and Mandal [26] introduced the AP method, which was subsequently used to investigate the quantum optical properties of diverse quantum systems (See, e.g., [27]). The AP method has demonstrated superior performance in comparison to the standard short-length approximation (SLA) method (See, e.g., [26]). The quantum mechanical description of the current two-waveguide system can be expressed using the momentum operator shown below [28].

$$\begin{aligned}\hat{G} = {} & \hbar k_1\hat{a}_1^\dagger\hat{a}_1 + \hbar k_2\hat{a}_2^\dagger\hat{a}_2 + \hbar k_b\hat{b}^\dagger\hat{b} + \hbar k_c\hat{c}^\dagger\hat{c} + \hbar k_d\hat{d}^\dagger\hat{d} + \hbar g\hat{a}_1\hat{b}^\dagger\hat{c}^\dagger + \hbar g\hat{a}_1^\dagger\hat{b}\hat{c} \\ & + \hbar\chi\hat{a}_1\hat{c}\hat{d}^\dagger + \hbar\chi\hat{a}_1^\dagger\hat{c}^\dagger\hat{d} + \hbar\kappa\hat{a}_2\hat{a}_1^\dagger + \hbar\kappa\hat{a}_2^\dagger\hat{a}_1\end{aligned} \tag{1}$$

On the right side of Eq. (1), the term $\hbar k_1\hat{a}_1^\dagger\hat{a}_1 + \hbar k_2\hat{a}_2^\dagger\hat{a}_2$ account for the pump modes in the first and the second waveguide, respectively. The term $\hbar k_b\hat{b}^\dagger\hat{b} + \hbar k_c\hat{c}^\dagger\hat{c} + \hbar k_d\hat{d}^\dagger\hat{d}$ accounts for the Stokes mode, the phonon mode, and the anti-Stokes mode, respectively, with k_j being the wavenumber of each mode. The term $\hbar g\hat{a}_1\hat{b}^\dagger\hat{c}^\dagger + \hbar g\hat{a}_1^\dagger\hat{b}\hat{c}$ represents the Stokes Raman scattering, where g is the Stokes nonlinear coefficient that governs this process. Inversely, the term $\hbar\chi\hat{a}_1\hat{c}\hat{d}^\dagger + \hbar\chi\hat{a}_1^\dagger\hat{c}^\dagger\hat{d}$ denotes anti-Stokes Raman scattering, which produces the anti-Raman mode by annihilating the pump and phonon modes; the governing parameter for this process is χ (The anti-Stokes nonlinear coefficient). Finally, the evanescent linear coupling between the fundamental modes is expressed by the last term in $\hbar\kappa\hat{a}_2\hat{a}_1{}^\dagger + \hbar\kappa\hat{a}_2{}^\dagger\hat{a}_1$. The strength of this coupling is proportional to the evanescent coupling coefficient κ, which is inversely proportional to the waveguide separation.

In the Heisenberg picture, the system is characterized by the spatial evolution of the quantum operators while the state vector remains constant. By inserting the momentum operator from Eq. (1) into the Heisenberg equation of motion $d\hat{a}_j/dz = (i/\hbar)[\hat{a}_j, \hat{G}]$, we arrive at the following set of coupled differential equations describing the spatial evolution of the quantum operators $\hat{a}_1, \hat{a}_2, \hat{b}, \hat{c}, and\ \hat{d}$.

$$\frac{d\hat{a}_1}{dz} = i\left(k_1\hat{a}_1 + g\hat{b}\hat{c} + \chi\hat{c}^\dagger\hat{d} + \kappa\hat{a}_2\right) \tag{2}$$

$$\frac{d\hat{a}_2}{dz} = i\left(k_2\hat{a}_2 + \kappa\hat{a}_1\right) \tag{3}$$

$$\frac{d\hat{b}}{dz} = i\left(k_b\hat{b} + g\hat{a}_1\hat{c}^\dagger\right) \tag{4}$$

$$\frac{d\hat{c}}{dz} = i\left(k_c\hat{c} + g\hat{a}_1\hat{b}^\dagger + \chi\hat{a}_1{}^\dagger\hat{d}\right) \tag{5}$$

$$\frac{d\hat{d}}{dz} = i\left(k_d\hat{d} + \chi\hat{a}_1\hat{c}\right) \tag{6}$$

In the AP method, the solution of these equations is assumed in the form of the Baker-Campbell-Hausdorff (BCH) formula, $\hat{a}_j(z) = exp\left[\frac{iz\hat{G}(z)}{\hbar}\right]\hat{a}_j(0)\, exp\left[\frac{-iz\hat{G}(z)}{\hbar}\right]$, which can be expanded as:

$$\hat{a}_j = \hat{a}_j(0) + \frac{iz}{\hbar}\left[\hat{G},\hat{a}_j(0)\right] - \frac{1}{2}\frac{z^2}{\hbar^2}\left[\hat{G},\left[\hat{G},\hat{a}_j(0)\right]\right] + \ldots \tag{7}$$

In the traditional short-length approximation (SLA) method, the commutator elements in Eq. (7) are evaluated, and a closed analytical solution is obtained for each operator, which contains terms up to z^2 only. This solution disregards numerous physical system insights [29]. Alternatively, the AP method proposed a more general solution of the form.

$$\hat{a}_1(z) = A_1(z)\hat{a}_1(0) + A_2(z)\hat{a}_2(0) + A_3(z)\hat{b}(0)\hat{c}(0) + A_4(z)\hat{c}^\dagger(0)\hat{d}(0) \tag{8}$$

$$\hat{a}_2(z) = B_1(z)\hat{a}_2(0) + B_2(z)\hat{a}_1(0) + B_3(z)\hat{b}(0)\hat{c}(0) + B_4(z)\hat{c}^\dagger(0)\hat{d}(0) \tag{9}$$

$$\hat{b}(z) = P_1(z)\hat{b}(0) + P_2(z)\hat{a}_2(0)\hat{c}^\dagger(0) + P_3(z)\hat{a}_1(0)\hat{c}^\dagger(0) \tag{10}$$

$$\hat{c}(z) = Q_1(z)\hat{c}(0) + Q_2(z)\hat{a}_2(0)\hat{b}^\dagger(0) + Q_3(z)\hat{a}_2{}^\dagger(0)\hat{d}(0) + Q_4(z)\hat{a}_1(0)\hat{b}^\dagger(0) + Q_5(z)\hat{a}_1{}^\dagger(0)\hat{d}(0) \tag{11}$$

$$\hat{d}(z) = R_1(z)\hat{d}(0) + R_2(z)\hat{a}_2(0)\hat{c}(0) + R_3(z)\hat{a}_1(0)\hat{c}(0) \tag{12}$$

The spatial evolution of the operators $\hat{a}_1(z)$, $\hat{a}_2(z)$, $\hat{b}(z)$, $\hat{c}(z)$ along the *z*-axis is described by the previous solutions (8)-(12) stated in terms of the unknown spatial-dependent coefficients $A_k(z)$, $B_k(z)$, $P_k(z)$, $Q_k(z)$ and $R_k(z)$ which assume to contain all *z* terms ranging from z^0 to z^∞. Substituting the operator solutions Eqs. (8)-(12) into each equation of motion in the set (2)-(6) and gathering similar terms from both sides produces a set of differential equations that characterize the spatial evolution of these unknown coefficients.

$$\frac{dA_1}{dz}=i\left(k_1A_1+\kappa B_2\right) \tag{13}$$

$$\frac{dA_2}{dz}=i\left(k_1A_2+\kappa B_1\right) \tag{14}$$

$$\frac{dA_3}{dz}=i\left(k_1A_3+gP_1Q_1+\kappa B_3\right) \tag{15}$$

$$\frac{dA_4}{dz}=i\left(k_1A_4+\chi Q_1^*R_1+\kappa B_4\right) \tag{16}$$

$$\frac{dB_1}{dz}=i\left(k_2B_1+\kappa A_2\right) \tag{17}$$

$$\frac{dB_2}{dz}=i\left(k_2B_2+\kappa A_1\right) \tag{18}$$

$$\frac{dB_3}{dz}=i\left(k_2B_3+\kappa A_3\right) \tag{19}$$

$$\frac{dB_4}{dz}=i\left(k_2B_4+\kappa A_4\right) \tag{20}$$

$$\frac{dP_1}{dz}=ik_bP_1 \tag{21}$$

$$\frac{dP_2}{dz}=i\left(k_bP_2+gA_2Q_1^*\right) \tag{22}$$

$$\frac{dP_3}{dz}=i\left(k_bP_3+gA_1Q_1^*\right) \tag{23}$$

$$\frac{dQ_1}{dz}=ik_cQ_1 \tag{24}$$

$$\frac{dQ_2}{dz}=i\left(k_cQ_2+gA_2P_1^*\right) \tag{25}$$

$$\frac{dQ_3}{dz}=i\left(k_cQ_3+\chi A_2^*R_1\right) \tag{26}$$

$$\frac{dQ_4}{dz} = i\left(k_c Q_4 + gA_1 P_1^*\right) \tag{27}$$

$$\frac{dQ_5}{dz} = i\left(k_c Q_5 + \chi A_1^* R_1\right) \tag{28}$$

$$\frac{dR_1}{dz} = ik_d R_1 \tag{29}$$

$$\frac{dR_2}{dz} = i\left(k_d R_2 + \chi A_2 Q_1\right) \tag{30}$$

$$\frac{dR_3}{dz} = i\left(k_d R_3 + \chi A_1 Q_1\right) \tag{31}$$

2.1. Criteria for Entanglement

Entanglement is defined by a set of criteria that determine its properties. These criteria assist in defining and identifying entanglement in quantum systems, and they have been tested in quantum physics experiments. In the literature, there are approximately twelve basic entanglement criteria. For entanglement detection, each criterion takes advantage of a distinct property of entangled systems, such as superposition, nonseparability, measurement correlations, entropy, and Bell's Inequality [30, 31]. Here, we will utilize the Hillery-Zubairy criteria to detect entanglement in the current system. These criteria were proposed by Hillery and Zubairy in 2006 [32] and are particularly applicable to systems with continuous variables, such as two-mode harmonic oscillators. The first criterion (HZ-I) tests the negativity, while the second (HZ-II) tests the nonseparability of the system. The HZ criteria have been employed to identify the entanglement in various quantum systems such as two-level atomic medium and optical nonlinear coupler (See e.g., [33]). Here we will utilize the HZ-I criterion to determine the presence of entanglement generated between the two fundamental modes propagating in both waveguides. In this case, the HZ-I criterion can be expressed as follows.

$$\varepsilon_I = \left\langle \hat{N}_1 \hat{N}_2 \right\rangle - |\langle \hat{a}_1 \hat{a}_2^\dagger \rangle|^2 < 0 \tag{32}$$

In the previous expression, ε_I represents the entanglement and $\hat{N} = \hat{a}^\dagger \hat{a}$ is the number operator. Substituting the operator solutions from Eqs. (8) and (9) into the Hillery-Zubairy criterion Eq. (32) results in the following formula for quantum entanglement between both fundamental modes given in terms of the previously defined spatial-dependent coefficients $A_k(z)$, $B_k(z)$, $P_k(z)$, $Q_k(z)$ and $R_k(z)$.

$$
\begin{aligned}
\varepsilon_I^{1,2} = & -|A_1|^2|B_2|^2 - |A_2|^2|B_1|^2 - A_1A_2^*B_1B_2^* - A_1^*A_2B_1^*B_2 - |A_1|^2|B_2|^2|\alpha_1|^2 - |A_2|^2|B_1|^2|\alpha_2|^2 \\
& -|A_1|^2 B_1^*B_2\alpha_1\alpha_2^* - |A_2|^2 B_1B_2^*\alpha_1^*\alpha_2 - |B_1|^2 A_1A_2^*\alpha_1\alpha_2^* - |B_2|^2 A_1^*A_2\alpha_1^*\alpha_2 - A_1A_2^*B_1B_2^*|\alpha_1|^2 \\
& -A_1^*A_2B_1^*B_2|\alpha_2|^2 - |A_1|^2 B_2B_3^*\alpha_1\alpha_b^*\alpha_c^* - |A_1|^2 B_2B_4^*\alpha_1\alpha_c\alpha_d^* - |A_2|^2 B_1B_3^*\alpha_2\alpha_b^*\alpha_c^* \\
& -|A_2|^2 B_1B_4^*\alpha_2\alpha_c\alpha_d^* - |B_1|^2 A_2^*A_3\alpha_2^*\alpha_b\alpha_c - |B_1|^2 A_2^*A_4\alpha_2^*\alpha_c^*\alpha_d - |B_2|^2 A_1^*A_3\alpha_1^*\alpha_b\alpha_c \\
& -|B_2|^2 A_1^*A_4\alpha_1^*\alpha_c^*\alpha_d - A_1A_2^*B_1B_3^*\alpha_1\alpha_b^*\alpha_c^* - A_1A_2^*B_1B_4^*\alpha_1\alpha_c\alpha_d^* - A_1^*A_2B_2B_3^*\alpha_2\alpha_b^*\alpha_c^* \\
& -A_1^*A_2B_2B_4^*\alpha_2\alpha_c\alpha_d^* - A_1^*A_3B_1^*B_2\alpha_2^*\alpha_b\alpha_c - A_2^*A_3B_1B_2^*\alpha_1^*\alpha_b\alpha_c - A_1^*A_4B_1^*B_2\alpha_2^*\alpha_c^*\alpha_d \\
& -A_2^*A_4B_1B_2^*\alpha_1^*\alpha_c^*\alpha_d
\end{aligned}
\tag{33}
$$

In the former expression (Eq. 33), α_j is the classical equivalent of the quantum operators $\hat{a}_j(0)$ at their initial state, i.e., at z = 0; it is the initial complex amplitude of a mode in a coherent state. Eq. 33 describes the evolution of the entanglement between the fundamental modes in the current Raman coupler system as a function of the interaction distance inside the waveguides.

3. Results

The numerical procedure consists of two major steps: (i) solving the coupled set of Eqs. (13)-(31) simultaneously to obtain numerical values of the spatial-dependent coefficients $A_k(z)$, $B_k(z)$, $P_k(z)$, $Q_k(z)$ and $R_k(z)$, and (ii) evaluating the entanglement using the criteria given by Eq. (33). However, from the numerical simulation perspective, putting the relevant equations in dimensionless form makes it easier to acquire numerical solutions. Here, we can scale the coupled system Eqs. (13)-(31) by dividing both sides of each equation by the wavenumber of the first mode k_1. Thus, a new set of differential equations with these dimensionless parameters $\tilde{k}_1 = k_1/k_1$, $\tilde{k}_2 = k_2/k_1$, $\tilde{k}_b = k_b/k_1$, $\tilde{k}_c = k_c/k_1$, $\tilde{k}_d = k_d/k_1$, $\tilde{g} = g/k_1$, $\tilde{\chi} = \chi/k_1$ and $\tilde{\kappa} = \kappa/k_1$ are obtained. In this case, the system evolves as a function of a scaled spatial distance given by $\tilde{z} = k_1 z$.

Figure 2 depicts the entanglement as a function of scaled distance in the stimulated Raman process, where the starting amplitude of each mode is nonzero. For the spontaneous process, where $\alpha_b = \alpha_c = \alpha_d = 0$, the same outcome as in Figure 2 is produced. Hence it is not presented here. The input parameters are $\alpha_1 = 10$, $\alpha_2 = 10$, $\alpha_b = 8$, $\alpha_c = 0.01$, $\alpha_d = 9$, $\tilde{k}_1 = 10$, $\tilde{k}_2 = 10$, $\tilde{k}_b = 10$, $\tilde{k}_c = 0.00001$, $\tilde{k}_d = 10$, $\tilde{g} = \tilde{\chi} = 0.0001$ and $\tilde{\kappa} = 0.8$. As can be seen in Figure 2, there is evidence of entanglement up to a value of $\tilde{z} \approx 1.5$. After that value, there is no indication of entanglement, and the graph continues to oscillate within the positive zone.

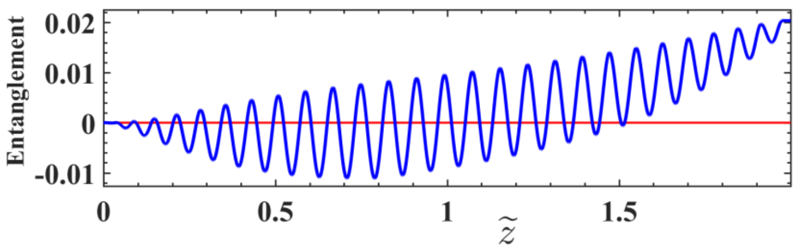

Fig. 2. Entanglement as a function of scaled distance $\tilde{z}$ in the case of the stimulated Raman process

When waveguides are in close proximity, the evanescent fields associated with the guided modes can extend beyond the boundaries of their respective waveguides. This can result in an overlap of the evanescent fields, leading to a coupling between the modes. The strength of mode coupling between neighboring waveguides depends on various factors, including the distance between the waveguides, their geometries, the characteristics of the modes, and the spatial extent of the evanescent fields. In this model, the strength of this kind of coupling is quantified by the coefficient $\tilde{\kappa}$. The influence of linear coupling coefficient $\tilde{\kappa}$ on the generated entangled states is depicted in Figure 3. For this purpose, the spatial evolution of entanglement is depicted for $\tilde{\kappa}$ = 0.01 in Figure 3(a), $\tilde{\kappa}$ = 0.5 in Figure 3(b), and $\tilde{\kappa}$ = 0.7 in Figure 3(c). We observe that the range of entanglement between both modes along the distance $\tilde{z}$ reduces with increasing the value of the linear coupling coefficient $\tilde{\kappa}$. When $\tilde{\kappa}$ = 0.01, 0.5, and 0.7, the entangled states evolve approximately up to a scaled distance of $\tilde{z}$ = 2.629, $\tilde{z}$ = 2.177, and $\tilde{z}$ = 1.696, respectively. On the other hand, when the linear coupling becomes stronger, the degree of entanglement (The negativity) becomes more significant. It should be noted that the mode coupling between adjacent waveguides could be controlled by Designing waveguide structures with appropriate spacing, isolation, and coupling mechanisms (see, e.g., [34, 35]).

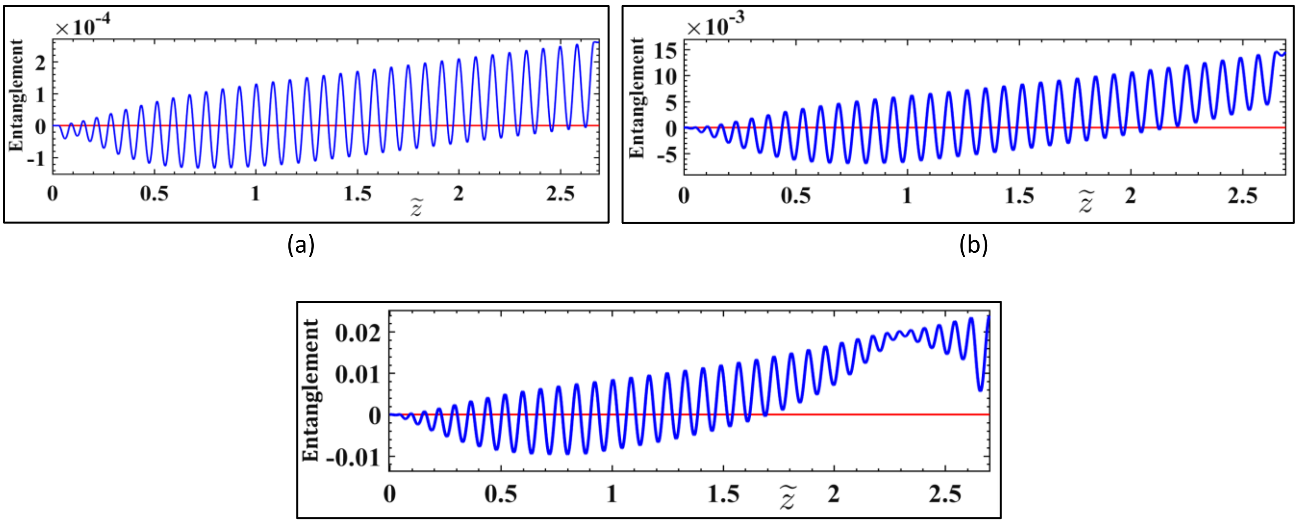

(a) (b)

(c)

Fig. 3. Entanglement as a function of scaled distance $\tilde{z}$ at different mode coupling constants. Other parameters remain as in Figure 2 (a) $\tilde{\kappa} = 0.01$, (b) $\tilde{\kappa} = 0.5$ (c) $\tilde{\kappa} = 0.7$

To investigate the effect of frequency-mismatching between the propagating modes on entanglement, we fixed the wavenumber of the first pump mode at $\tilde{k}_1 = 10$, while the wavenumber for the second pump mode $\tilde{k}_2$ is increased gradually. For this purpose, the spatial evolution of entanglement is depicted for three different values of mismatching; Figure 4(a) for $\Delta\tilde{k} = \tilde{k}_2 - \tilde{k}_1 = 12 - 10 = 2$, Figure 4(b) for $\Delta\tilde{k} = \tilde{k}_2 - \tilde{k}_1 = 14 - 10 = 4$, and Figure 4(c) for $\Delta\tilde{k} = \tilde{k}_2 - \tilde{k}_1 = 23 - 10 = 13$. In these three figures, we observe a gradual improvement in the range of entanglement and its frequency. In the usual situation, where two modes coexist in the same waveguide, frequency-mismatched modes can interfere with each other. Constructive or destructive interference effects can lead to changes in the amplitude or the phase of the modes. This kind of unwanted mode coupling can lead to cross-talk, signal degradation, or loss in performance.

However, in this case of a directional coupler, the two modes are in different waveguides but placed close to each other, and the light is coupled to facilitate efficient energy transfer. When we increase the frequency of a propagating light mode, the wavelength decreases, and the energy increase since the energy of a photon is directly proportional to its frequency. Thus, fixing the frequency of one mode while increasing the frequency of the other mode leads to a stronger crossing coupling. As the frequency of one mode increases, while the other remains fixed, the energy is gradually transferred to the mode with the increasing frequency. Initially, when the frequency difference between the two modes is small, the energy transfer is minimal (Figure 4(a)), and each mode predominantly propagates in its respective waveguide without significant interaction. However, as the frequency difference increases, the coupling between the modes becomes more pronounced, leading to a transfer of energy between the waveguides (Figure 4(b) and 4(c)). The phenomenon of mode coupling in a directional coupler has applications in various fields, such as integrated optics, optical communications, and photonic circuits, where the control and manipulation of light propagation paths are essential.

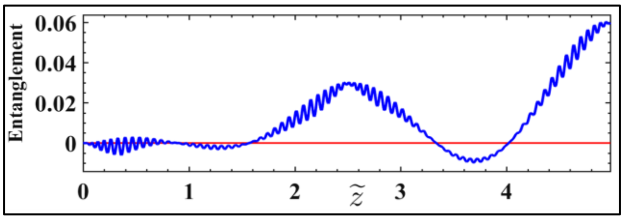

(a)

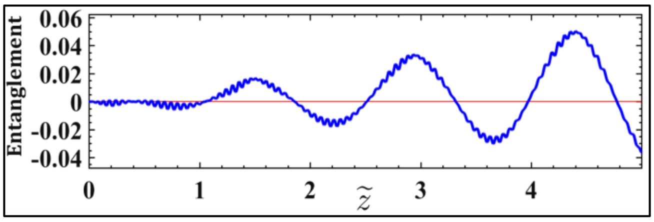

(b)

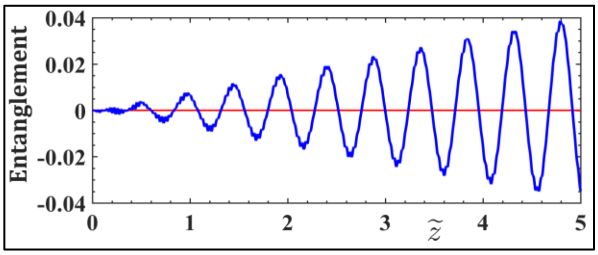

(c)

Fig. 4. Generated entanglement in case of frequency mismatching. The first mode wavenumber is fixed at $\tilde{k}_1 = 10$ while the second mode wavenumber $\tilde{k}_2$ is increased. Other parameters remain as in Figure 2
(a) $\tilde{k}_2 = 12$, (b) $\tilde{k}_2 = 14$ and (c) $\tilde{k}_2 = 23$

4. Conclusion

In conclusion, the analytical-perturbative method has been utilized to study the generation of entangled states in the Raman nonlinear coupler. The Heisenberg equation of motion was used to describe the evolution of the momentum operator of the current system. The solution of the system is obtained by utilizing the weak pump field approximation, which disregards terms with higher power of the nonlinear coefficient beyond the second order. The Hillery-Zubairy criterion is used to evaluate the possible quantum entanglement. The study has been centred around the establishment of entanglement between the two fundamental pump modes in the waveguides. The findings indicate a consistent entanglement that persists until reaching a specific interaction distance. As the linear coupling parameter increases, the maximum reachable distance for entanglement decreases, even though the degree of entanglement improves. It is observed that there is a rapid fluctuation of entanglement when there is a high value of frequency mismatching between both modes.

Acknowledgments
Abdel-Baset M. A. Ibrahim gratefully acknowledges the financial support provided by the Malaysia Ministry of Higher Education (MOHE) under the national grant FRGS/1/2021/STG07/UITM/02/10.

References

[1] Mahavidyalaya, Badrinarayan Barwale. "Consequences and limitations of conventional computers and their solutions through quantum computers." *Leonardo Electronic Journal of Practices and Technologies* 19 (2011): 161-171.

[2] Sharma, Meenakshi, and Sonia Thind. "A Quantum key distribution technique using quantum cryptography." In *Research Anthology on Blockchain Technology in Business, Healthcare, Education, and Government*, p. 263-271. IGI Global, 2021. https://doi.org/10.4018/978-1-7998-5351-0.ch016

[3] Ursin, Rupert, Felix Tiefenbacher, T. Schmitt-Manderbach, Henning Weier, Thomas Scheidl, M. Lindenthal, Bibiane Blauensteiner, T. Jennewein, J. Perdigues, P. Trojek, B. Ömer, M. Fürst, M. Meyenburg, J. Rarity, Z. Sodnik, C. Barbieri, H. Weinfurter, and A. Zeilinger. "Entanglement-based quantum communication over 144 km." *Nature Physics* 3, no. 7 (2007): 481-486. https://doi.org/10.1038/nphys629

[4] Zhang, Chang-Yue, and Zhu-Jun Zheng. "Entanglement-based quantum key distribution with untrusted third party." *Quantum Information Processing* 20 (2021): 1-20. https://doi.org/10.1007/s11128-021-03080-6

[5] Zhahir, Amirul Asyraf, Siti Munirah Mohd, Mohd Ilias M. Shuhud, Bahari Idrus, Hishamuddin Zainuddin, Nurhidaya Mohamad Jan, and Mohamed Ridza Wahiddin. "Quantum computing and its application." *International Journal of Advanced Research in Technology and Innovation* 4, no. 1 (2022): 55-65. https://doi.org/10.55057/ijarti.2022.4.1.7

[6] King, Brennan Michael. "The viability of quantum computing." *Missouri S&t's Peer to Peer* 2, no. 1 (2018): 5.

[7] Alam, Nasir, Kishore Thapliyal, Anirban Pathak, Biswajit Sen, Amit Verma, and Swapan Mandal. "Bose-condensed optomechanical-like system and a Fabry–Perot cavity with one movable mirror: Quantum correlations from the perspectives of quantum optics." *The European Physical Journal D* 73 (2019): 1-12. https://doi.org/10.1140/epjd/e2019-90448-x

[8] Wu, Ling-An, Min Xiao, and H. J. Kimble. "Squeezed states of light from an optical parametric oscillator." *JOSA B* 4, no. 10 (1987): 1465-1475. https://doi.org/10.1364/JOSAB.4.001465

[9] Julius, Rafael, Abdel-Baset MA Ibrahim, Hichem Eleuch, and Pankaj K. Choudhury. "Sub-Poissonian photon squeezing and entanglement in optical chain second harmonic generation." *Journal of Modern Optics* 66, no. 10 (2019): 1129-1138. https://doi.org/10.1080/09500340.2019.1603408

[10] Julius, Rafael, Mansoor Zahirzai, Abdel-Baset MA Ibrahim, Hichem Eleuch, and Pankaj K. Choudhury. "Single-and compound-mode squeezing in nonlinear coupler with frequency mismatch." *Journal of Electromagnetic Waves and Applications* 34, no. 3 (2020): 301-315. https://doi.org/10.1080/09205071.2019.1702591

[11] Hanapi, Mohd Syafiq M., Abdel-Baset MA Ibrahim, Rafael Julius, and Pankaj Kumar Choudhury. "Squeezed Light Generation in three-channel nonlinear coupler with second-harmonic generation and frequency mismatch." In *Journal of Physics: Conference Series*, 2411, no. 1, p. 012021. IOP Publishing, 2022. https://doi.org/10.1088/1742-6596/2411/1/012021

[12] Hanapi, Mohd Syafiq M., Abdel-Baset Ibrahim, Rafael Julius, Pankaj K. Choudhury, and Hichem Eleuch. "Nonclassical light in a three-waveguide coupler with second-order nonlinearity." *EPJ Quantum Technology* 11, no. 1 (2024): 1-23. https://doi.org/10.1140/epjqt/s40507-024-00263-9

[13] Julius, Rafael, Abdel-Baset MA Ibrahim, Pankaj Kumar Choudhury, and Hichem Eleuch. "Quantum states generation in multichannel directional coupler with second-order nonlinearity." *Optik* 186 (2019): 212-220. https://doi.org/10.1016/j.ijleo.2019.03.027

[14] Julius, Rafael, Abdel-Baset MA Ibrahim, Mohd Kamil Abd-Rahman, and P. K. Choudhury. "Quantum dynamics of a four-channel Kerr nonlinear directional coupler." *Optical Review* 25, no. 5 (2018): 563-570. https://doi.org/10.1007/s10043-018-0448-x

[15] Julius, Rafael, Abdel-Baset MA Ibrahim, Pankaj Kumar Choudhury, and Hichem Eleuch. "On the nonclassical dynamics of cavity-assisted four-channel nonlinear coupler." *Chinese Physics B* 27, no. 11 (2018): https://doi.org/114206.10.1088/1674-1056/27/11/114206

[16] Julius, Rafael, Abdel-Baset MA Ibrahim, and Mohd SM Deni. "Quantum state generation in a four-mode Kerr nonlinear directional coupler." *Laser Physics* 24, no. 3 (2014): 035202. https://doi.org/10.1088/1054-660X/24/3/035202

[17] Ibrahim, Abdel-Baset MA, B. A. Umarov, and M. R. B. Wahiddin. "Squeezing in the Kerr nonlinear coupler via phase-space representation." *Physical Review A* 61, no. 4 (2000): 043804. https://doi.org/10.1103/PhysRevA.61.043804

[18] Hanapi, Mohd Syafiq M., Abdel-Baset MA Ibrahim, and P. K. Choudhury. "On the perturbative approach to analyse entanglement in two-channel Kerr nonlinear coupler." *Optik* 243 (2021): 167420. https://doi.org/10.1016/j.ijleo.2021.167420

[19] Hanapi, Mohd Syafiq M., Abdel-Baset MA Ibrahim, and Rafael Julius. "On the Detection of Single-Mode Squeezed States in Kerr Nonlinear Coupler." In *Journal of Physics: Conference Series* 2075, no. 1, p. 012002. IOP Publishing, 2021. https://doi.org/10.1088/1742-6596/2075/1/012002

[20] Hanapi, Mohd Syafiq M., Abdel-Baset MA Ibrahim, Rafael Julius, and Hichem Eleuch. "Quantum Kerr nonlinear coupler: analytical versus phase-space method." *Canadian Journal of Physics* 99, no. 999 (2021): 832-840. https://doi.org/10.1139/cjp-2020-0389

[21] Bache, Morten, Yu B. Gaididei, and Peter Leth Christiansen. "Nonclassical statistics of intracavity coupled χ (2) waveguides: the quantum optical dimer." *Physical Review A* 67, no. 4 (2003): 043802. https://doi.org/10.1103/PhysRevA.67.043802

[22] Shipp, Dustin W., Faris Sinjab, and Ioan Notingher. "Raman spectroscopy: Techniques and applications in the life sciences." *Advances in Optics and Photonics* 9, no. 2 (2017): 315-428. https://doi.org/10.1364/AOP.9.000315

[23] Thapliyal, Kishore, Anirban Pathak, Biswajit Sen, and Jan Peřina. "Lower-and higher-order nonclassical features in non-degenerate hyper-Raman processes." *Optics Communications* 444 (2019): 111-119. https://doi.org/10.1016/j.optcom.2019.03.044

[24] Perina Jr, J., and and J. Perina. "Statistics of light in Raman and Brillouin nonlinear couplers." *Quantum and Semiclassical Optics: Journal of the European Optical Society Part B* 9, no. 3 (1997): 443. https://doi.org/10.1088/1355-5111/9/3/013

[25] Das, Moumita, Kishore Thapliyal, Biswajit Sen, Jan Peřina, and Anirban Pathak. "Interplay between quantum Zeno and anti-Zeno effects in a nondegenerate hyper-Raman nonlinear optical coupler." *Physical Review A* 103, no. 1 (2021): 013713. https://doi.org/10.1103/PhysRevA.103.013713

[26] Sen, Biswajit, and Swapan Mandal*. "Squeezed states in spontaneous Raman and in stimulated Raman processes." *Journal of Modern Optics* 52, no. 13 (2005): 1789-1807. https://doi.org/10.1080/09500340500072984

[27] Thapliyal, Kishore, Anirban Pathak, and Jan Peřina. "Linear and nonlinear quantum Zeno and anti-Zeno effects in a nonlinear optical coupler." *Physical Review A* 93, no. 2 (2016): 022107. https://doi.org/10.1103/PhysRevA.93.022107

[28] Perina, J., and J. Perina Jr. "Quantum statistical properties of codirectional and contradirectional nonlinear couplers with phase mismatch." *Quantum and Semiclassical Optics: Journal of the European Optical Society Part B* 7, no. 5 (1995): 863. https://doi.org/10.1088/1355-5111/7/5/008

[29] Peřina, J., and J. Bajer. "Non-classical light in nonlinear symmetric and asymmetric couplers." *Journal of Modern Optics* 42, no. 11 (1995): 2337-2346. https://doi.org/10.1080/09500349514552031

[30] Sumairi, AiniSyahida, S. N. Hazmin, and CH Raymond Ooi. "Quantum entanglement criteria." *Journal of Modern Optics* 60, no. 7 (2013): 589-597. https://doi.org/10.1080/09500340.2013.796016

[31] Zhahir, Amirul Asyraf, Siti Munirah Mohd, Mohd Ilias M. Shuhud, Bahari Idrus, Hishamuddin Zainuddin, Nurhidaya Mohamad Jan, and Mohamed Ridza Wahiddin. "Entanglement detection: A scoping review." *Journal of Advanced Research in Applied Sciences and Engineering Technology* 42, no. 2 (2024): 209-220. https://doi.org/10.37934/araset.42.2.209220

[32] Hillery, Mark, and M. Suhail Zubairy. "Entanglement conditions for two-mode states: Applications." *Physical Review A-Atomic, Molecular, and Optical Physics* 74, no. 3 (2006): 032333. https://doi.org/10.1103/PhysRevA.74.032333

[33] Thapliyal, Kishore, Anirban Pathak, Biswajit Sen, and Jan Peřina. "Higher-order nonclassicalities in a codirectional nonlinear optical coupler: Quantum entanglement, squeezing, and antibunching." *Physical Review A* 90, no. 1 (2014): 013808. https://doi.org/10.1103/PhysRevA.90.013808

[34] Cheng, Zhang-Ying, Xuan-Dong Liu, Le-Chen Ma, and Ming Chen. "Developing highly efficient and electric-field-sensitive fiber-waveguide evanescent couplers." *Applied Optics* 60, no. 17 (2021): 5087-5093. https://doi.org/10.1364/AO.424746

[35] Gibson, Brant C., and Peter M. Dower. "Fiber evanescent field power maximization via refractive index design." In *ACOFT/AOS 2006-Australian Conference on Optical Fibre Technology/Australian Optical Society*, pp. 66-68. IEEE, 2006. https://doi.org/10.1109/ACOFT.2006.4519268